JBC Papers in Press. Published on May 2, 2018 as Manuscript RA118.002592
The latest version is at http://www.jbc.org/cgi/doi/10.1074/jbc.RA118.002592

Methionine biosynthesis and transport are functionally redundant for the growth and virulence of *Salmonella* Typhimurium

Asma Ul Husna[1], Nancy Wang[1*], Simon A. Cobbold[2], Hayley J. Newton[1], Dianna M. Hocking[1], Jonathan J. Wilksch[1], Timothy A. Scott[1#], Mark R. Davies[1], Jay C. Hinton[3], Jai J. Tree[1,4], Trevor Lithgow[5], Malcolm J. McConville[2^], Richard A. Strugnell[1*^]

[1]Department of Microbiology and Immunology, The University of Melbourne at The Peter Doherty Institute for Infection and Immunity, Parkville, Victoria, Australia; [2]Department of Biochemistry and Molecular Biology, The University of Melbourne at the Bio21 Institute, Parkville, Victoria, Australia; [3]Institute of Integrative Biology, University of Liverpool, UK; [4]School of Biotechnology and Biomolecular Sciences, University of New South Wales, Sydney, Australia; [5]Department of Microbiology, Monash University, Clayton, Victoria, Australia.
^contributed equally as co-senior authors.

Running Title: Methionine in *Salmonella* Typhimurium virulence

[#]Present address: Department of Pathogen Molecular Biology, London School of Hygiene and Tropical Medicine, London, UK.

*To whom correspondence should be addressed:
Richard A. Strugnell: Department of Microbiology and Immunology, The University of Melbourne at Peter Doherty Institute for Infection and Immunity, Parkville, Victoria, Australia; rastru@unimelb.edu.au; Tel: +61 3 8344 8479; Fax: +61 3 9347 1540.
Nancy Wang: Department of Microbiology and Immunology, The University of Melbourne at Peter Doherty Institute for Infection and Immunity, Parkville, Victoria, Australia; nancyw@unimelb.edu.au; Tel +61 3 8344 9918.

Keywords: methionine; S-adenosyl methionine (SAM); biosynthesis; transporter; virulence; *in vivo* infection; *Salmonella enterica*; peptidoglycan.

ABSTRACT

Methionine (Met) is an amino acid essential for many important cellular and biosynthetic functions, including the initiation of protein synthesis and *S*-adenosylmethionine-mediated methylation of proteins, RNA, and DNA. The *de novo* biosynthetic pathway of Met is well conserved across prokaryotes but absent from vertebrates, making it a plausible antimicrobial target. Using a systematic approach, we examined the essentiality of *de novo* methionine biosynthesis in *Salmonella enterica* serovar Typhimurium, a bacterial pathogen causing significant gastrointestinal and systemic diseases in humans and agricultural animals. Our data demonstrates that Met biosynthesis is essential for *S.* Typhimurium to grow in synthetic media and within cultured epithelial cells where Met is depleted in the environment. During systemic infection of mice, the virulence of *S.* Typhimurium was not affected when either *de novo* Met biosynthesis or high-affinity Met transport was disrupted alone, but when disrupted in combination led to severe *in vivo* growth attenuation, demonstrating a functional redundancy between *de novo* biosynthesis and acquisition as a mechanism of sourcing Met to support growth and virulence for *S.* Typhimurium during infection. In addition, our LC-MS analysis revealed global changes in the metabolome of *S.* Typhimurium mutants lacking Met biosynthesis, and also uncovered unexpected interactions between Met and peptidoglycan biosynthesis. Together, this study highlights the complexity of the interactions between a single amino acid, Met, and other bacterial processes leading to virulence in the host, and indicates that disrupting the *de novo* biosynthetic pathway alone

is likely to be ineffective as an antimicrobial therapy against *S.* Typhimurium.

INTRODUCTION

Methionine (Met) is a sulphur-containing proteinogenic amino acid that is required for the initiation of protein synthesis (1). S-adenosyl methionine (SAM), a downstream derivative of Met, acts as a major methyl donor in the cell and methylates a variety of macromolecules such as DNA, RNA, protein and lipids (2). A *de novo* pathway for Met biosynthesis is present in the vast majority of prokaryotes, albeit with variations in the enzymes that drive the biosynthetic cascade (3,4). In contrast, the full *de novo* Met biosynthesis is absent from vertebrates, which must obtain this amino acid through external sources such as diet and gut flora (5,6). In recent years, it has been increasingly recognised that central metabolism represents a promising yet underexploited area for the development of antimicrobial drugs (7). The apparent essentiality in microbes and absence in mammals makes the Met biosynthetic pathway an especially attractive target for antimicrobial therapy.

Salmonella enterica is a Gram-negative, facultative intracellular bacterium which causes gastrointestinal and systemic diseases in animals and humans. There are approximately 2500 serovars in this species which include the human-adapted enteric fever pathogens *S. enterica* var. Typhi and Paratyphi, and invasive non-typhoidal *Salmonella* (iNTS), alongside serovars that cause debilitating gastroenteritis, including *S. enterica* var. Typhimurium (8,9). For all *Salmonella* serovars, the capacity to grow in the host is central to bacterial virulence (10). In mammalian hosts, *S. enterica* grows in the blood and reticuloendothelial system largely within a defined, membrane-bound endocytic compartment called the *Salmonella*-containing vacuole (SCV) (11,12). The extent to which *S. enterica* salvages essential nutrients from the lumen of the SCV and the nutrient composition of this vacuole remains poorly defined, and the micronutrient environment of the SCV has not been fully resolved. *Ex vivo*, *S. enterica* is capable of growth in minimal media containing glucose as a carbon source, and key ions, and the metabolic potential of this species has been recognised and mapped (13). It is less clear though how this considerable capability is exploited for maximal growth *in vivo*. The essentiality of the pathways can only be determined by systematic analysis *in vitro* and in animal models, and fine mapping is required to determine whether essential pathways contain novel targets for antibiotic development.

The *de novo* biosynthetic pathway for Met has been previously reported in *S. enterica* (Fig. 1). This pathway is regulated by the transcription factors MetJ and MetR (14). With its co-repressor SAM, MetJ represses the transcription of all *met* genes except *metH* (15). In contrast, MetR is an autoregulated transcriptional activator that controls the expression of *metA*, *metF, metE*, *metH*, (16). In addition to *de novo* biosynthesis, *S. enterica* is able to acquire Met from extracellular sources through a high-affinity transporter that is encoded by the *metD* locus, encoding an ATP Binding Cassette (ABC) transporter composed of three subunits: the ATPase (MetN), a transmembrane permease (MetI) and a periplasmic Met binding protein (MetQ). Biochemical analysis has shown that MetNIQ transports both the D- and L-enantiomers of Met (17,18). In the absence of the high-affinity MetNIQ transporter system, genetic analysis has suggested that *S. enterica* is able to transport Met at much lower affinity, through a putative and cryptic low-affinity Met transporter system termed 'MetP' (19-21). In contrast to MetNIQ, MetP transports L-Met but not D-Met, and the coding gene(s) for MetP remains unidentified to-date.

S. enterica may encounter markedly different nutrient levels during local (e.g. the gut) and systemic (e.g. the spleen and liver) infections which, in turn, may vary the bacterium's dependence on *de novo* biosynthesis and nutrient import pathways for growth in different tissue niches. The enzymes required for Met biosynthesis and the Met transporter have been implicated in the virulence of *S. enterica* and other bacteria (22-28). However, these pathways have not been systematically investigated for their role in the virulence of *S. enterica*. The aim of this study was to investigate the essentiality of *de novo* biosynthesis and transport of Met in the growth and virulence of *S.* Typhimurium *in vitro* and *in vivo*.

Results

In vitro validation of the Met biosynthetic pathway in S. Typhimurium and growth of defined Met auxotrophs in mice

Previous transcriptional analyses of *S.* Typhimurium grown in media and in tissue culture cells have demonstrated that the genes involved in the *de novo* Met synthesis pathway (*metA*, *metB*, *metC*, *metE*, *metF* and *metH*) are expressed under a

variety of growth conditions (Supplementary Fig. S1, deduced from (29)). While the expression level of the *de novo* pathway is relatively low in rich media, much stronger expression was observed under growth conditions where the *Salmonella* Pathogenicity Island-2 (SPI-2) genes were expressed, or when the bacteria were inside macrophages (30).

Defined mutants in the Met biosynthetic pathway: Δ*metA*, Δ*metB*, Δ*metC*, Δ*metE,* Δ*metF*, Δ*metH* and Δ*metE*Δ*metH*, were generated in *S.* Typhimurium SL1344, sequenced and tested for their ability to grow in M9 minimal media, with or without added L-Met, and in nutrient-rich media (LB). All mutants grew in LB media at a rate comparable to wild-type SL1344 (data not shown). In M9 minimal media supplemented with Met, Met mutants grew as efficiently as SL1344 over a 24-hour period (Fig. 2A), suggesting that the absence of the *de novo* biosynthetic pathway was compensated by the transport of exogenously available Met. As expected, the Δ*metA*, Δ*metB*, Δ*metC*, Δ*metE* and Δ*metF* mutants exhibited Met auxotrophy in M9 media whereas Δ*metH* showed substantial growth over the 24-hour period (Fig. 2A), confirming that MetH is not essential for *de novo* biosynthesis of Met under aerobic conditions (31,32). The growth of the Δ*metH* mutant in M9 media was apparently supported by a functional Met synthase, i.e. MetE, as Δ*metE*Δ*metH* failed to grow in M9 media in the absence of exogenous Met (Fig. 2A). It has been suggested that the functionality of MetH in *E. coli* is vitamin B12-dependent (33). To test whether there is an equivalent dependence in *S.* Typhimurium, Δ*metE*, Δ*metH* and Δ*metE*Δ*metH* mutants were grown in M9 media with or without vitamin B12. All three mutants grew in the presence of vitamin B12 (Fig. 2B). The Δ*metE* mutant, which was dependent on MetH to synthesise Met, grew only when vitamin B12 was added (Fig. 2B), confirming that MetH activity in *S.* Typhimurium is vitamin B12-dependent. As *S.* Typhimurium synthesises vitamin B12 only under anaerobic conditions (31), growth of the Δ*metE* mutant in M9 media should have been restored when oxygen was depleted. Indeed, Δ*metE,* Δ*metH* and Δ*metE*Δ*metH* both grew in M9 media under anaerobic conditions and phenocopied their growth in M9 media with vitamin B12 under aerobic conditions (Fig. 2C). These observations are consistent with an understanding that *S.* Typhimurium synthesises vitamin B12 under anaerobic conditions, and support a level of functional redundancy between MetE and MetH during *de novo* biosynthesis of Met in *S.* Typhimurium.

To assess the requirement for *de novo* Met synthesis for intracellular bacterial growth, HeLa cells were infected with *S.* Typhimurium wild-type and mutants, and the intracellular bacterial load was assessed after 2, 5 and 10 hours. When HeLa cells were cultivated in DMEM growth media lacking Met, the intracellular growth of Δ*metA*, Δ*metB*, Δ*metC* and Δ*metF* was significantly attenuated compared with the wild-type control (Fig. 2D). The Δ*metE* mutant only showed obvious growth after 5 hours. In contrast, the Δ*metH* mutant showed intracellular growth comparable to SL1344, suggesting that a functional MetE is sufficient for supporting intracellular replication in the SCV (Fig. 2D). Importantly, when HeLa cells were cultivated in DMEM containing physiological levels of L-Met, none of the mutants showed any significant defect in intracellular growth (Supplementary Fig. S2), demonstrating that exogenous Met can rescue Met auxotrophy, presumably reflecting direct or indirect transport of Met from the culture media to the lumen of the bacterial-occupied SCV.

Previous reports have proposed that Met biosynthesis might be required for virulence of *S.* Typhimurium in mice or chickens (24,34). To test this requirement in mice, the virulence of individual *de novo* biosynthetic mutants was studied in C57BL/6 mice, in which wild-type SL1344 is fully virulent and invariably results in a systemic, lethal infection (35,36). Groups of mice were infected with 200 cfu of the different Met auxotrophic mutants intravenously and, at day 5 post-infection, mice were culled and the bacterial load in the liver (Fig. 2E) and spleen (Fig. 2F) was determined by viable count. The number of bacteria recovered from mice infected with the mutants was comparable to those from mice infected with SL1344. Hence, none of the mutants showed virulence defects in mice following intravenous infection. Another group of mice were infected orally with Δ*metB*, Δ*metE,* Δ*metH* or Δ*metE*Δ*metH*. The bacterial load in the spleen and liver of mice infected with the mutant strains was comparable to those from mice infected with the wild-type *S.* Typhimurium (Supplementary Fig. S3). These data showed that *de novo* Met biosynthesis is not essential for the growth of *S.* Typhimurium in C57BL/6 mice, regardless of the route of infection.

Met auxotrophs deficient in the high-affinity transporter (MetNIQ) are attenuated in mice

Our observation that *S.* Typhimurium mutants were able to grow intracellularly and *in vivo* without a functional *de novo* Met biosynthetic pathway suggested that Met acquisition via the transporters may play an important role in bacterial virulence. To test this hypothesis, a high-affinity transporter mutant of *S.* Typhimurium, Δ*metNIQ*, was constructed. As expected, the Δ*metNIQ* mutant grew in M9 minimal media in the absence of Met supplementation (Fig. 3A), suggesting that the high-affinity Met transporter is not essential for growth in M9 media provided that *de novo* synthesis is intact.

To determine whether dual mutations in *de novo* biosynthesis and the high-affinity transporter of Met affected the growth of *S.* Typhimurium *in vitro* and *in vivo*, Δ*metNIQ*Δ*metEH* and Δ*metNIQ*Δ*metB* mutants were generated. As expected, the Δ*metNIQ*Δ*metEH* and Δ*metNIQ*Δ*metB* mutants were unable to grow in M9 minimal media without added Met (Fig. 3B); this Met auxotrophy confirms that a combined deficiency in both biosynthesis and high-affinity transport is inhibitive for growth. Interestingly, the addition of L-Met into M9 media restored the growth of all these mutant strains, consistent with the presence and activity of the putative and functional low-affinity transporter 'MetP' (19,20). Hence, this data supports the theory that MetP activity enables sufficient Met uptake to facilitate efficient growth *in vitro*.

To determine whether the observed *in vitro* growth attenuation was reflected by reduced growth of *S.* Typhimurium inside mammalian cells, Δ*metNIQ*, Δ*metNIQ*Δ*metB* and Δ*metNIQ*Δ*metEH* mutants were used to infect HeLa cells in Met-free DMEM. Whereas Δ*metNIQ* mutant was capable of intracellular growth to a level similar to SL1344 over a 10-hour period, Δ*metNIQ*Δ*metB* and Δ*metNIQ*Δ*metEH* mutants were unable to grow (Fig. 3C, top row). The presence of L-Met in DMEM fully restored the growth of the mutant strains in HeLa cells (Fig. 3C, bottom row), suggesting that the activity of the cryptic transporter MetP was sufficient to support intracellular growth in HeLa cells.

To determine whether dual mutations in *de novo* biosynthesis and high-affinity transporter of Met reduced *S.* Typhimurium virulence *in vivo*, C57BL/6 mice were intravenously infected with Δ*metNIQ*, Δ*metNIQ*Δ*metB* and Δ*metNIQ*Δ*metEH* mutant strains or whild-type. At day 5 post-infection, mice infected with Δ*metNIQ* had a similarly high bacterial load in the liver (Fig. 3D) and spleen (Fig. 3E) and comparable with that of SL1344-infected mice, indicating that loss of the high-affinity Met transporter alone does not reduce *S.* Typhimurium virulence *in vivo*. In contrast, infection with Δ*metNIQ*Δ*metB* and Δ*metNIQ*Δ*metEH* mutants resulted in a significantly reduced bacterial load in the liver (Fig. 3D) and spleen (Fig. 3E), and this attenuation was reversed when the Δ*metNIQ*Δ*metB* mutant was complemented by *metB* (Fig. 3D and E). Similar results were obtained when the Δ*metNIQ*Δ*metB* and Δ*metNIQ*Δ*metEH* mutants were used to infect mice via the oral route (Supplementary Fig. S4), confirming that Δ*metNIQ*Δ*metB* and Δ*metNIQ*Δ*metEH* are attenuated in mice regardless of the route of infection. Taken together, these results demonstrate that restriction of Met availability has a strong impact on the virulence of *S.* Typhimurium *in vivo*, and the presence of the putative cryptic transporter (MetP) alone is insufficient to sustain maximal bacterial growth in the permissive murine host.

Metabolite profiling in S. Typhimurium Met biosynthetic and high-affinity transporter mutants

To further define the impact of Met pathway gene disruptions on bacterial metabolism, *S.* Typhimurium wild-type and mutants lacking either or both of the *de novo* biosynthesis pathway and the high-affinity Met transporter were grown in LB media, and polar metabolites were extracted and analysed by liquid chromatography-mass spectrometry (LC-MS). The intracellular accumulation of 5-methyl-tetrahydropteroyltri-L-glutamate, a member of the polyglutamate forms of 5-methyltetrahydrofolate (37), was significantly increased in Δ*metH* (~10 fold) and further increased in Δ*metNIQ*Δ*metEH* (~25 fold), but not in Δ*metE*, compared with SL1344 (Fig. 4). This result suggests that both MetE and MetH are functionally active as *S.* Typhimurium grew in LB broth, but MetH is either more abundant, or more efficient in the formation of 5-methyltetrahydrofolate. On the other hand, the Δ*metB* mutant exhibited a significantly elevated pool of O-succinylhomoserine compared to the wild-type, consistent with a defect in the MetB catalysed conversion of O-succinylhomoserine to cystathionine (Fig. 4).

An untargeted mass/charge (m/z) feature analysis of the mutant lines led to the identification of a number of unexpected metabolite changes. Pair-wise comparisons were performed to identify differences that were statistically different ($p<0.05$) and to filter interesting m/z features. Deletion of *metB* led to significant increases in the intracellular levels of SAM (5.5-fold increase compared to wild-type), and a number of other metabolites including glycerate, adenine, hexose-6-phosphate, 3-phosphoglycerate and gluconate were also increased compared to the wild-type (Fig. 5A and Table 3). By comparison, Δ*metE* did not show any significantly different m/z features (Fig. 5B) whereas only the m/z feature corresponding to 5-methyl-tetrahydropteroyltri-L-glutamate, a representative form of 5-methyltetrahydrofolate, was significantly different in the Δ*metH* mutant (Fig. 5C).

Interestingly, several m/z features corresponding to peptidoglycan biosynthetic intermediates were significantly different for the Δ*metB* mutant, including UDP-N-acetyl-muraminate-alanine-glutamate (Fig. 5D). This, in turn, suggested an association between Met biosynthesis and peptidoglycan biosynthesis. Disruption of *metB* led to a decrease in intracellular concentrations of UDP-N-acetyl-muraminate (~0.4-fold) and a large increase of UDP-N-acetyl-muramoyl-L-alanine (12-fold), UDP-N-acetyl-muramoyl-L-alanyl-D-glutamate (1400-fold) and UDP-N-acetyl-muramoyl-L-alanyl-D-γ-glutamyl-*meso*-2,6-diaminopimelate (4-fold) (Fig. 5D). A decrease in UDP-N-acetyl-muraminate and an increase in UDP-N-acetyl-muramoyl-L-alanine (9-fold), UDP-N-acetyl-muramoyl-L-alanyl-D-glutamate (1000-fold) and UDP-N-acetyl-muramoyl-L-alanyl-D-γ-glutamyl-*meso*-2,6-diaminopimelate (5-fold) was also observed in the double mutant Δ*metNIQ*Δ*metB* (Fig. 5D).

Ex vivo, the Δ*metB* mutant had a reduced growth rate compared with the wild-type in bile salts. To study the impact of the altered levels of peptidoglycan-related metabolites, the Δ*metB* mutant and wild-type were tested in LB broth in the presence of EDTA, SDS, lysozyme, fasted state simulated intestinal fluid (FaSSIF), but no significant differences in growth were found (Supplementary Table S1). A small increase (~2 mm on 15 mm) in β-lactam antibiotic sensitivity, using a validated disc sensitivity method, was observed for the Δ*metB* mutant (data not shown). In addition, when the Δ*metB* and wild-type were tested in MacConkey broth supplemented with 0.6% bile salt a small but consistent delay in the growth of Δ*metB* was observed (Supplementary Figure S5).

Discussion

There is increased interest in identifying metabolic pathways in bacterial pathogens, which are essential and distinct from those in their mammalian and human hosts, as potential antibiotic targets (38-42). Previous studies suggested that perhaps 400 *S. enterica* enzymes are dispensable and that essential pathways are often protected against random mutation by redundancy, reflecting the selective pressure placed on metabolism as a key virulence trait (13). Met biosynthesis and transport is an important part of the interconnected and interdependent amino acid metabolism (43). In this study, the essentiality of Met biosynthesis and transport in the mammalian virulence of *S.* Typhimurium was investigated.

We showed that *de novo* Met biosynthesis is not essential when the bacteria are able to obtain Met from their environment. The growth rate of the bacteria with or without *de novo* Met biosynthesis appeared similar in Met-rich media (e.g. LB broth), suggesting that transport systems can compensate for the loss of *de novo* biosynthesis. Met biosynthetic mutants requires the presence of Met in the culture media in order to grow inside of HeLa cells (Fig. 2D and Supplementary Fig. S2), suggesting that extracellular Met becomes available to bacteria in the SCV within a few hours of infection. It is likely that Met is relatively abundant in the SCV during *in vivo* infection, as all of the Met biosynthetic mutants were as virulent as wild-type *S.* Typhimurium in mice (Fig. 2E and F), presumably because the Met acquisition systems have access to a sufficient source of Met for supporting bacterial growth in the infected animal.

It is only when *de novo* biosynthesis and high-affinity transport of Met are both disrupted that we observed severe growth attenuation in HeLa cells (Fig. 3C) and importantly, in infected mice (Fig. 3D and E). This result strongly suggests functional redundancy between transport and biosynthesis as a source of Met for *S.* Typhimurium inside of the host. Whether Met is acquired (e.g. Δ*metB*) or synthesised (e.g. Δ*metNIQ*Δ*metB* and Δ*metNIQ*Δ*metB* complemented with *metB*), the growth *in vivo* appears to be comparable, suggesting that either *de novo* biosynthesis or the high-affinity transport system of Met alone can

provide Met in excess to what is required for *S.* Typhimurium to grow at maximal capacity in the host. Hence, at least in the case of *S.* Typhimurium, it is probably quite difficult to inhibit growth by targeting the Met biosynthetic pathway. The observation that Δ*metNIQ*Δ*metB* and Δ*metNIQ*Δ*metEH* were still able to grow in mice is suggestive of a Met acquisition system independent of MetNIQ, which is consistent with the presence of a low-affinity transporter MetP (19,20). Hence, our study also provides additional support for the presence of a putative, low-affinity transporter 'MetP', which has yet to be identified.

Our description of this apparent redundancy between *de novo* synthesis and high-affinity transport of Met conflicted with previous studies that showed Met auxotrophs are defective for intracellular survival in macrophages and epithelial cells (22,23), and have reduced virulence in mice (24,28) and in 1-day old chickens (34). This may be at least in part due to differences in the study design. In our study, C57BL/6 mice were infected with a single strain; whereas previous studies typically using competition assays (i.e. infecting the same host with wild-type and mutant strains), which may put more pressure on the mutant to grow in the competitive environment. It is not uncommon to have divergent results from single infections and competitive infections (44,45). Another study has shown that the *S.* Typhimurium lacking the high-affinity transporter MetNIQ is attenuated in C3H/HeN mice (25). C3H/HeN mice carry the resistant allele of *Nramp1*, which controls Fe^{3+} availability in the phagosome and is a major determinant of murine susceptibility to *S.* Typhimurium; consequently C3H/HeN mice are much more resistant to *S.* Typhimurium infection than the *Nramp1* deficient C57BL/6 mice (46,47). It is possible that the differences in attenuation observed in earlier studies, but not ours, relate to differences in genetic susceptibility of the mice. Finally, earlier animal studies did not complement the bacterial Met mutation, nor sequence the mutant strains, and it is possible that secondary mutations, not mutations in Met biosynthesis *per se*, were responsible for the observed attenuation in mice.

To generate novel insights about the Met biosynthesis pathway in *S.* Typhimurium, the changes in bacterial concentrations of key metabolites was examined by LC-MS (Fig. 4 and 5). Mass spectrometry revealed substrate accumulation in Met biosynthetic mutants Δ*metB*, Δ*metE*, Δ*metH* and the high-affinity transporter mutant Δ*metNIQ,* and mutants deficient in both (Δ*metNIQ*Δ*metB* and Δ*metNIQ*Δ*metEH*). This analysis revalidated the pathway model for Met biosynthesis shown in Fig. 1, which has been proposed since the 1980s but to the best of our knowledge, has not been systematically studied in *S. enterica* until now.

The observed accumulation of substrates provides interesting insights into the kinetics of enzyme activities. The deletion of both Met synthases (i.e. Δ*metNIQ*Δ*metEH*) leads to a profound difference in 5-methyltetrahydrofolate concentration, a metabolite in the one-carbon cycle (Fig. 4). In the Δ*metH* mutant, there is a 10-fold higher intracellular concentration of the substrate compared to Δ*metE*, indicating that MetE is much less efficient than MetH, supporting previous findings (48). Presumably, perturbation of the one-carbon cycle led to an accumulation of homocysteine, which is toxic for bacterial cells (49,50). This is probably why we consistently observed that Δ*metNIQ*Δ*metEH* grew slower *in vivo* compared to Δ*metNIQ*Δ*metB* (Fig. 3, Supplementary Fig. S4).

The disruption of the *metB* gene led to several unexpected observations. Firstly, the intracellular pool of SAM was increased in Δ*metB* compared with wild-type (Fig. 4), indicating a defect in SAM catabolism following perturbation of the activated methyl cycle in this mutant. This observation argues that, in the Δ*metB* mutant, homocysteine, which is converted into SAM, cannot be derived through *de novo* biosynthesis in Δ*metB*, hence is not fed into the activated methyl cycle. Further comparisons of the LC-MS/MS data between Δ*metB* and SL1344 revealed differences in many metabolites from disparate pathways; how disruption to a single enzyme in Met biosynthesis caused perturbations in other pathways was unclear but the data demonstrates the complexity of modelling intracellular metabolite fluxes in bacteria. Interestingly, this analysis revealed that the concentration of several metabolites linked with peptidoglycan synthesis, were grossly increased in Δ*metB* and Δ*metNIQ*Δ*metB* (Fig. 5D). *Enterobacteriaceae* peptidoglycan usually consists of alternating molecules of N-acetyl-glucosamine and N-acetyl-muramic acid that are linked by a tetrapeptide of L-alanine, D-glutamate, diaminopimelic acid (DAP) and D-alanine. Because Met biosynthesis and *m*-DAP biosynthesis are linked through aspartate metabolism (43), and

L-cystathionine can substitute for DAP (51), the perturbation of the intracellular metabolite pools related to Met biosynthesis might also impact peptidoglycan synthesis. While LC-MS revealed significant changes in the levels of peptidoglycan intermediates, these changes were not reflected by increased sensitivity to agents, e.g. β-lactam antibiotics, which act through peptidoglycan synthesis, or directly on peptidoglycan, with the exception of growth in bile. Bile is known to remodel *S. enterica* peptidoglycan (52). However, it is recognised that *Enterobacteriaceae* with altered cell wall physiology are very robust. For example, *E. coli* with decreased *m*-DAP, which reduced the peptidoglycan density by 50%, did not show any detectable alteration in morphology or growth characteristics (53).

The data obtained from the LC-MS analysis with the complemented mutant Δ*metNIQ*Δ*metB* (Fig. 4 and 5) suggested that complementation by pACYC184*metB* did not fully restore the metabolite levels seen in the Δ*metNIQ* mutant. However, this is not unusual since, as related, genetic complementation using a plasmid will differ from the native level due to plasmid copy number and regulation, accounting for the partially complemented phenomena that is observed.

This study supports earlier models of *S. enterica* metabolism that have suggested significant redundancy in key pathways linked with growth (13). The research reported here was a systematic analysis of Met metabolism in response to earlier investigations, which suggested that Met auxotrophy was attenuating for bacterial growth in animals, and that *de novo* Met metabolism might therefore provide new antibiotic targets. The regulation of Met synthesis, a complex regulon comprising MetR and MetJ (16,54), was not investigated since the aim of the study was to determine the essentiality of *de novo* Met synthesis in *in vivo* growth. We found that mutants unable to synthesise Met efficiently obtained the amino acid from their intracellular niche via their high-affinity Met transporter, suggesting that the SCV contains sufficient Met to sustain normal bacterial growth even in the absence of *de novo* synthesis. Severe reductions in virulence *in vivo* was only observed when both *de novo* Met biosynthesis and high-affinity Met transport were lost. The impact of mutations in the Met biosynthesis and transporter genes on other pathways was revealed, reaffirming the complexity of the bacterial metabolome and the interactions between metabolites that have yet to be mapped. Considerably more basic science on bacterial metabolism will be needed to identify novel, functionally non-redundant targets.

Experimental procedures

Bacterial strains and growth conditions

The bacterial strains and plasmids used in this study are listed in Table 1. All mutant strains were constructed on the *S.* Typhimurium SL1344 genetic background and SL1344 was used as the wild-type strain in all experiments. The SL1344 strain has been described previously (36); its virulence is well defined and is resistant to streptomycin. Appropriate antibiotics, including streptomycin (50 μg/ml) chloramphenicol (30 μg/ml), kanamycin (50 μg/ml) and ampicillin (100 μg/ml) were added to growth media as required. To obtain mid-exponential growth phase, *S.* Typhimurium and *E. coli* strains were grown in 10 ml Luria-Bertani (LB) broth (BD Difco) overnight, and 100 μl of the overnight culture was subcultured into 10 ml fresh LB broth, and grown with shaking (180 rpm) at 37ºC for 3-4 hours until the optical density reading at 600 nm reached 0.6-0.8. Growth phenotypes were characterised in LB broth or M9 minimal media (2 mM $MgSO_4$, 0.1 mM $CaCl_2$, 0.4% glucose, 8.5 mM NaCl, 42 mM Na_2HPO_4, 22 mM KH_2PO_4, 18.6 mM NH_4Cl and 100 μM histidine). Met or vitamin B12 was supplemented at 100 μM. For assessing growth under anaerobic conditions, cultures were grown shaking in air-tight jars with AnaeroGen (ThermoFisher) for depletion of oxygen.

Construction of strains and plasmids

Defined deletions of sequence encoding the *met* biosynthesis genes *metA*, *metB*, *metC*, *metE*, *metF*, *metH* and Met high-affinity transporter *metNIQ* were generated in *S.* Typhimurium SL1344. The biosynthetic mutant and high-affinity transporter mutant were combined together to generate the double mutant Δ*metNIQ*Δ*metB* and the triple mutant Δ*metNIQ*Δ*metEH.* The double mutant Δ*metNIQ*Δ*metB* was complemented by introducing the *de novo* biosynthetic *metB* gene into Δ*metNIQ*Δ*metB* strain in *trans*. This strain is named as Δ*metNIQ*Δ*metB* pACYC184*metB*. Gene deletions and concomitant insertions of an antibiotic resistance cassette were constructed using a Lambda Red-mediated 'gene gorging' method (55). All constructs were verified by PCR and moved to a SL1344 or relevant background via P22 phage transduction (36,56). Primers used to

construct mutants are listed in Table 2. Genetic complementation of mutant Δ*metNIQ*Δ*metB* was achieved by cloning *metB* into pACYC184 via the *Bam*HI and *Sal*I sites and then introducing pACYC184*metB* into the Δ*metNIQ*Δ*metB* mutant. All constructs were verified by restriction analysis and DNA sequencing. Key mutants were also sequenced using Illumina whole genome sequencing and analysed using the pipeline at the Wellcome Sanger Institute, Hinxton, UK.

Infection of epithelial cells

Infection of HeLa cells (sourced from American Type Culture Collection (ATCC)) was conducted using established gentamicin protection assay protocols (57,58). Briefly, HeLa cells were grown in DMEM supplemented with 10% fetal calf serum (FCS) and 2 mM L-glutamax (Life Technologies), in a humidified 37°C, 5% CO_2 incubator. One day prior to infection, HeLa cells were seeded in 24-well plates at 2×10^5 cells per well. *S.* Typhimurium strains were grown to mid-exponential phase prior and frozen in LB with 10% glycerol at -80°C. Bacteria were thawed immediately before infection, washed in antibiotic-free tissue culture media and diluted in DMEM media with or without L-Met, then added to HeLa cell monolayers at a multiplicity of infection (MOI) of 5-10. The cfu in the inoculum was estimated by plating on LB agar plates. Infected HeLa cells were centrifuged at 600 × *g* for 5 min immediately after the addition of bacteria and then incubated for 1 hour at 37°C. After 1 hour, the tissue culture media was replaced with DMEM media with or without Met and containing 100 μg/ml of gentamicin to kill extracellular bacteria. The concentration of gentamicin was reduced to 10 μg/ml at 2 hours post-infection and maintained for the remainder of the experiment. To enumerate intracellular bacteria, cells were washed twice with PBS, and lysed with 1% Triton X-100 (Sigma) for 15 min to release the intracellular bacteria. The bacteria were enumerated by plating appropriate dilutions on LB agar plates.

Ethics Statement

All animal research conducted in this study was approved by the Animal Ethics Committee (Biochemistry & Molecular Biology, Dental Science, Medicine, Microbiology & Immunology) at The University of Melbourne, under project number 1413141. All experiments were conducted in accordance with the Australian Code of Practice for the Care and Use of Animals for Scientific Purposes, 8th edition 2013.

Mouse infections

Age- and sex-matched C57BL/6 mice were used between 6-8 weeks of age, to assess the virulence of mutant strains, using either the intravenous or oral route of infection. For intravenous infections, 200 cfu of each bacterial strain was prepared in 200 μl PBS and injected into the lateral tail vein. For oral infections, mice were orally gavaged with 100 μl 10% sodium bicarbonate immediately before oral gavage of 200 μl containing approximately 5×10^7 cfu of *S.* Typhimurium strains. To prepare the inoculum, all strains of *S.* Typhimurium were grown shaking at 180 rpm in M9 minimal media supplemented with 100 μM Met, at 37ºC for 24 hours, and stored in 10% glycerol at -80ºC until use. Immediately prior to infection, the stored aliquots were thawed and diluted in PBS to the required concentration. At designated time points post-infection, the spleen and liver were removed aseptically, homogenated using the Stomacher 80 Biomaster paddle blender (Seward), and serial dilutions were plated on LB agar plates with streptomycin to determine the bacterial load.

Preparation of stock solutions and standards for Liquid Chromatography-Mass Spectrometry (LC-MS)

Stock solutions of the related underivatized metabolites were prepared at 1.0 mg/ml in an appropriate solvent. Before using, the solutions were combined and diluted with water to give an appropriate standard metabolite mix solution. $^{13}C^{15}N$-Aspartate (Cambridge Bioscience) was used as an Internal Standard at 1 μM in Milli-Q water. All stock solutions were stored at -20ºC.

Sample harvest (metabolic arrest) for LC-MS

Each *S.* Typhimurium strain was grown at 37°C to mid-exponential phase in 10 ml LB, with shaking at 180 rpm. The culture was diluted into 30 ml PBS, and chilled in an ice/water slurry for 5 min and subsequently centrifuged (931 ×*g*, 1ºC, 10 min). The pellet was then washed in 1 ml PBS and centrifuged (17,295 × *g*). This washing step was repeated before removing the PBS and storing the cell pellet at -80ºC until metabolite extraction was performed.

Extraction of metabolites for LC-MS

Cell pellets were resuspended with 400 µl of 75% ethanol solution containing 1:1000 of Internal Standard. Cell lysis was ensured by repeated cycles of freeze-thaw, for a total of 10 times, while cooling to -80ºC. Cellular debris was pelleted by centrifugation (17,295 × g, 5 min, 1ºC). The metabolic extract was transferred to a new tube and stored at -80ºC until analysis.

Instrumentation

A SeQuant ZIC-pHILIC column (5 µM, 150 × 4.6 mm, Millipore) coupled to a 1260 series HPLC system (Agilent) was used to separate metabolites. The method used was previously described (59) with slight modifications: a flow rate of 0.3 mL/min with 20 mM ammonium carbonate in water and 100% acetonitrile was used as the mobile phase. A binary gradient was set up as follows: 0.5 min: 80% acetonitrile, 15.5 min: 50% acetonitrile, 17.5 min: 20% acetonitrile, 18.5 min: 5% acetonitrile, 21 min 5% acetonitrile, 23 min 80% acetonitrile and held at 80% acetonitrile until 29.5 min. Detection of metabolites was performed on an Agilent Q-TOF mass spectrometer 6545 operating in negative ESI mode. The scan range was 85-1200 m/z between 2 and 28.2 min at 0.8 spectra/sec.

Calibration and validation

LC-MS.d files were converted to .mzXML files using MS convert and analysed using the LCMS R package (60,61). Following alignment, groups were extracted with a mass window of 10 ppm and statistical analysis performed using MetaboAnalyst 3.0 (62). The dataset was uploaded, filtered using the interquartile range, log transformed, and a one-way ANOVA performed with Tukey's HSD ($p < 0.01$). Data was analysed using MAVEN in parallel to validate the LCMS results (63). Following alignment, metabolites were assigned using exact mass (<10 ppm) and retention time (compared to a standards library of 150 compounds run the same day). Scatter plots were generated for each pairwise comparison and statistical significance was determined using a *P* value < 0.05 with Benjamini correction.

Acknowledgements
The authors acknowledge the helpful advice of Dr. Peter Ayling. Sarah Baines assisted with the analysis of the whole genome sequences. Shruti Gujaran assisted with testing for antibiotic resistance in different bacterial strains.

Conflicts of interest
The authors declare that they have no conflicts of interest with the contents of this article.

Reference

1. Kozak M. Comparison of initiation of protein synthesis in procaryotes, eucaryotes, and organelles. Microbiol Rev. 1983 Mar;47(1):1–45.
2. Cantoni GL. Biological methylation: selected aspects. Annu Rev Biochem. 1975;44(1):435–51.
3. Kalan EB, Ceithaml J. Methionine biosynthesis in *Escherichia coli*. J Bacteriol. 1954 Sep;68(3):293–8.
4. Ferla MP, Patrick WM. Bacterial methionine biosynthesis. Microbiology. 2014 Aug 1;160(Pt_8):1571–84.
5. Morowitz MJ, Carlisle EM, Alverdy JC. Contributions of Intestinal Bacteria to Nutrition and Metabolism in the Critically Ill. Surg Clin North Am. 2011 Aug;91(4):771–85.
6. Neis E, Dejong C, Rensen S. The Role of Microbial Amino Acid Metabolism in Host Metabolism. Nutrients. 2015 Apr;7(4):2930–46.
7. Murima P, McKinney JD, Pethe K. Targeting bacterial central metabolism for drug development. Chemistry & Biology. 2014 Nov 20;21(11):1423–32.
8. Mastroeni P, Maskell D. *Salmonella* infections : clinical, immunological and molecular aspects. 2006. Available from: https://ezp.lib.unimelb.edu.au/login?url=https://search.ebscohost.com/login.aspx?direct=true&db=cat00006a&AN=melb.b3005900&site=eds-live&scope=site
9. Gordon MA. Invasive nontyphoidal Salmonella disease. Curr Opin Infect Dis. 2011 Oct;24(5):484–9.
10. Steeb B, Claudi B, Burton NA, Tienz P, Schmidt A, Farhan H, et al. Parallel Exploitation of Diverse Host Nutrients Enhances Salmonella Virulence. Nassif X, editor. PLoS Pathog. 2013 Apr 25;9(4):e1003301.
11. Knodler LA, Steele-Mortimer O. Taking possession: biogenesis of the Salmonella-containing vacuole. Traffic. 2003 Sep;4(9):587–99.
12. Steele-Mortimer O. The Salmonella-containing vacuole: moving with the times. Curr Opin Microbiol. 2008 Feb;11(1):38–45.
13. Becker D, Selbach M, Rollenhagen C, Ballmaier M, Meyer TF, Mann M, et al. Robust Salmonella metabolism limits possibilities for new antimicrobials. Nature. 2006 Mar 16;440(7082):303–7.
14. Somers WS, Phillips SE. Crystal structure of the met repressor-operator complex at 2.8 A resolution reveals DNA recognition by beta-strands. Nature. Nature Publishing Group; 1992 Oct 1;359(6394):387–93.
15. Old IG, Phillips SE, Stockley PG, Saint-Girons I. Regulation of methionine biosynthesis in the Enterobacteriaceae. Prog Biophys Mol Biol. 1991;56(3):145–85.
16. Maxon ME, Redfield B, Cai XY, Shoeman R, Fujita K, Fisher W, et al. Regulation of methionine synthesis in Escherichia coli: effect of the MetR protein on the expression of the metE and metR genes. Proc Natl Acad Sci USA. 1989;86(1):85–9.
17. Gál J, Szvetnik A, Schnell R, Kálmán M. The metD D-methionine transporter locus of Escherichia coli is an ABC transporter gene cluster. J Bacteriol. 2002 Sep;184(17):4930–2.
18. Merlin C, Gardiner G, Durand S, Masters M. The Escherichia coli metD locus encodes an ABC transporter which includes Abc (MetN), YaeE (MetI), and YaeC (MetQ). J Bacteriol [Internet]. 2002 Oct;184(19):5513–7. Available from: http://eutils.ncbi.nlm.nih.gov/entrez/eutils/elink.fcgi?dbfrom=pubmed&id=12218041&retmode=ref&cmd=prlinks
19. Ayling PD, Bridgeland ES. Methionine transport in wild-type and transport-defective mutants of Salmonella typhimurium. J Gen Microbiol. 1972 Nov;73(1):127–41.
20. Ayling PD, Mojica-a T, Klopotowski T. Methionine transport in Salmonella typhimurium: evidence for at least one low-affinity transport system. J Gen Microbiol. 1979 Oct;114(2):227–46.
21. Shaw NA, Ayling PD. Cloning of high-affinity methionine transport genes from Salmonella typhimurium. FEMS Microbiol Lett. 1991 Mar 1;62(2-3):127–31.

22. Fields PI, Swanson RV, Haidaris CG, Heffron F. Mutants of Salmonella typhimurium that cannot survive within the macrophage are avirulent. Proc Natl Acad Sci USA. National Academy of Sciences; 1986 Jul;83(14):5189–93.
23. Leung KY, Finlay BB. Intracellular replication is essential for the virulence of Salmonella typhimurium. Proc Natl Acad Sci USA. 1991 Dec 15;88(24):11470–4.
24. Ejim LJ, D'Costa VM, Elowe NH, Loredo-Osti JC, Malo D, Wright GD. Cystathionine beta-lyase is important for virulence of Salmonella enterica serovar Typhimurium. Infect Immun. 2004 Jun;72(6):3310–4.
25. Richardson AR, Payne EC, Younger N, Karlinsey JE, Thomas VC, Becker LA, et al. Multiple targets of nitric oxide in the tricarboxylic acid cycle of Salmonella enterica serovar typhimurium. Cell Host Microbe [Internet]. 2011 Jul 21;10(1):33–43. Available from: http://linkinghub.elsevier.com/retrieve/pii/S1931312811001946
26. Bogard RW, Davies BW, Mekalanos JJ. MetR-Regulated Vibrio cholerae Metabolism Is Required for Virulence. MBio. 2012 Aug 28;3(5):e00236–12–e00236–12.
27. Berney M, Berney-Meyer L, Wong K-W, Chen B, Chen M, Kim J, et al. Essential roles of methionine and S-adenosylmethionine in the autarkic lifestyle of Mycobacterium tuberculosis. Proc Natl Acad Sci USA. National Acad Sciences; 2015 Aug 11;112(32):10008–13.
28. Jelsbak L, Mortensen MIB, Kilstrup M, Olsen JE. The In Vitro Redundant Enzymes PurN and PurT Are Both Essential for Systemic Infection of Mice in Salmonella enterica Serovar Typhimurium. Infect Immun. 2016 Jul;84(7):2076–85.
29. Kröger C, Colgan A, Srikumar S, Händler K, Sivasankaran SK, Hammarlöf DL, et al. An infection-relevant transcriptomic compendium for Salmonella enterica Serovar Typhimurium. Cell Host Microbe [Internet]. 2013 Dec 11;14(6):683–95. Available from: http://bioinf.gen.tcd.ie/salcom/img/Kroger%20et%20al%202013%20-%20CellHost&Microbe%20-%20PUBLISHED%20VERSION.pdf
30. Srikumar S, Kröger C, Hébrard M, Colgan A, Owen SV, Sivasankaran SK, et al. RNA-seq Brings New Insights to the Intra-Macrophage Transcriptome of Salmonella Typhimurium. Miller SI, editor. PLoS Pathog. 2015 Nov 12;11(11):e1005262–26.
31. Jeter RM, Olivera BM, Roth JR. Salmonella typhimurium synthesizes cobalamin (vitamin B12) de novo under anaerobic growth conditions. J Bacteriol [Internet]. 1984 Jul;159(1):206–13. Available from: http://eutils.ncbi.nlm.nih.gov/entrez/eutils/elink.fcgi?dbfrom=pubmed&id=6376471&retmode=ref&cmd=prlinks
32. González JC, Banerjee RV, Huang S, Sumner JS, Matthews RG. Comparison of cobalamin-independent and cobalamin-dependent methionine synthases from Escherichia coli: two solutions to the same chemical problem. Biochem [Internet]. 1992 Jul 7;31(26):6045–56. Available from: http://eutils.ncbi.nlm.nih.gov/entrez/eutils/elink.fcgi?dbfrom=pubmed&id=1339288&retmode=ref&cmd=prlinks
33. Banerjee RV, Johnston NL, Sobeski JK, Datta P, Matthews RG. Cloning and sequence analysis of the Escherichia coli metH gene encoding cobalamin-dependent methionine synthase and isolation of a tryptic fragment containing the cobalamin-binding domain. J Biol Chem. 1989 Aug 15;264(23):13888–95.
34. Shah DH, Shringi S, Desai AR, Heo E-J, Park J-H, Chae J-S. Effect of metC mutation on Salmonella Gallinarum virulence and invasiveness in 1-day-old White Leghorn chickens. Vet Microbiol. 2007 Jan;119(2-4):352–7.
35. Wray C, Sojka WJ. Experimental Salmonella typhimurium infection in calves. Res Vet Sci [Internet]. 1978 Sep;25(2):139–43. Available from: http://eutils.ncbi.nlm.nih.gov/entrez/eutils/elink.fcgi?dbfrom=pubmed&id=364573&retmode=ref&cmd=prlinks
36. Hoiseth SK, Stocker BA. Aromatic-dependent Salmonella typhimurium are non-virulent and effective as live vaccines. Nature [Internet]. 1981 May 21;291(5812):238–9. Available from: http://eutils.ncbi.nlm.nih.gov/entrez/eutils/elink.fcgi?dbfrom=pubmed&id=7015147&retmode=ref&cmd=prlinks

37. Kwon YK, Lu W, Melamud E, Khanam N, Bognar A, Rabinowitz JD. A domino effect in antifolate drug action in Escherichia coli. Nat Chem Biol. 2008 Oct;4(10):602–8.
38. Coates ARM, Hu Y. Novel approaches to developing new antibiotics for bacterial infections. Br J Pharmacol. 2007 Dec;152(8):1147–54.
39. Harada E, Iida KI, Shiota S, Nakayama H, Yoshida SI. Glucose Metabolism in Legionella pneumophila: Dependence on the Entner-Doudoroff Pathway and Connection with Intracellular Bacterial Growth. J Bacteriol. 2010 May 11;192(11):2892–9.
40. Rossi M, Amaretti A, Raimondi S. Folate Production by Probiotic Bacteria. Nutrients. 2011 Dec;3(12):118–34.
41. Pitchandi P, Hopper W, Rao R. Comprehensive database of Chorismate synthase enzyme from shikimate pathway in pathogenic bacteria. BMC Pharmacol Toxicol. 2013 May 22;14(1):4.
42. Bourne C. Utility of the Biosynthetic Folate Pathway for Targets in Antimicrobial Discovery. Antibiotics. 2014 Mar;3(1):1–28.
43. Kanehisa M, Sato Y, Kawashima M, Furumichi M, Tanabe M. KEGG as a reference resource for gene and protein annotation. Nucleic Acids Res. 2016 Jan 3;44(D1):D457–62.
44. Beuzón CR, Holden DW. Use of mixed infections with Salmonella strains to study virulence genes and their interactions in vivo. Microbes Infect. 2001 Nov;3(14-15):1345–52.
45. Raman SB, Nguyen MH, Cheng S, Badrane H, Iczkowski KA, Wegener M, et al. A Competitive Infection Model of Hematogenously Disseminated Candidiasis in Mice Redefines the Role of Candida albicans IRS4in Pathogenesis. Deepe GS Jr., editor. Infect Immun. 2013 Apr 15;81(5):1430–8.
46. Lissner CR, Swanson RN, O'Brien AD. Genetic control of the innate resistance of mice to Salmonella typhimurium: expression of the Ity gene in peritoneal and splenic macrophages isolated in vitro. J Immunol. 1983 Dec;131(6):3006–13.
47. Nairz M, Fritsche G, Crouch M-LV, Barton HC, Fang FC, Weiss G. Slc11a1 limits intracellular growth of *Salmonella enterica* sv. Typhimurium by promoting macrophage immune effector functions and impairing bacterial iron acquisition. Cell Microbiol. 2009 Sep;11(9):1365–81.
48. Bertrand EM, Moran DM, McIlvin MR, Hoffman JM, Allen AE, Saito MA. Methionine synthase interreplacement in diatom cultures and communities: Implications for the persistence of B 12use by eukaryotic phytoplankton. 2013 Jun 14;58(4):1431–50. Available from: http://doi.wiley.com/10.4319/lo.2013.58.4.1431
49. Tuite NL, Fraser KR, O'Byrne CP. Homocysteine Toxicity in Escherichia coli Is Caused by a Perturbation of Branched-Chain Amino Acid Biosynthesis. 2005 Jun 20;187(13):4362–71. Available from: http://jb.asm.org/cgi/doi/10.1128/JB.187.13.4362-4371.2005
50. Sikora M, Jakubowski H. Homocysteine editing and growth inhibition in Escherichia coli. Microbiology. 2009 Jun 1;155(6):1858–65.
51. Richaud C, Mengin-Lecreulx D, Pochet S, Johnson EJ, Cohen GN, Marlière P. Directed evolution of biosynthetic pathways. Recruitment of cysteine thioethers for constructing the cell wall of Escherichia coli. J Biol Chem. 1993 Dec 25;268(36):26827–35.
52. Hernández SB, Cava F, Pucciarelli MG, García-del Portillo F, de Pedro MA, Casadesús J. Bile-induced peptidoglycan remodelling in *Salmonella enterica*. Environ Microbiol. 2015 Apr;17(4):1081–9.
53. Prats R, de Pedro MA. Normal growth and division of Escherichia coli with a reduced amount of murein. J Bacteriol. 1989 Jul;171(7):3740–5.
54. Augustus AM, Spicer LD. The MetJ regulon in gammaproteobacteria determined by comparative genomics methods. BMC Genomics. 2011 Nov 14;12(1):145.
55. Herring CD, Glasner JD, Blattner FR. Gene replacement without selection: regulated suppression of amber mutations in Escherichia coli. Gene [Internet]. 2003 Jun 5;311:153–63. Available from: http://eutils.ncbi.nlm.nih.gov/entrez/eutils/elink.fcgi?dbfrom=pubmed&id=12853150&retmode=ref&cmd=prlinks
56. Davis RW, Botstein D, Roth JR. Advanced bacterial genetics : a manual for genetic engineering. Cold Spring Harbor Laboratory; 1980.

57. Mandell GL. Interaction of intraleukocytic bacteria and antibiotics. J Clin Invest. 1973 Jul;52(7):1673–9.
58. Vaudaux P, Waldvogel FA. Gentamicin antibacterial activity in the presence of human polymorphonuclear leukocytes. Antimicrob Agents Chemother. 1979 Dec;16(6):743–9.
59. Cobbold SA, Chua HH, Nijagal B, Creek DJ, Ralph SA, McConville MJ. Metabolic Dysregulation Induced in Plasmodium falciparum by Dihydroartemisinin and Other Front-Line Antimalarial Drugs. J Infect Dis. 2016 Jan 15;213(2):276–86.
60. Smith CA, Want EJ, O'Maille G, Abagyan R, Siuzdak G. XCMS: processing mass spectrometry data for metabolite profiling using nonlinear peak alignment, matching, and identification. Anal Chem. 2006 Feb 1;78(3):779–87.
61. Tautenhahn R, Böttcher C, Neumann S. Highly sensitive feature detection for high resolution LC/MS. BMC Bioinformatics. 2008 Nov 28;9(1):504.
62. Xia J, Sinelnikov IV, Han B, Wishart DS. MetaboAnalyst 3.0—making metabolomics more meaningful. Nucleic Acids Res. 2015 Jun 30;43(W1):W251–7.
63. Clasquin MF, Melamud E, Rabinowitz JD. LC-MS data processing with MAVEN: a metabolomic analysis and visualization engine. Curr Protoc Bioinformatics. Hoboken, NJ, USA: John Wiley & Sons, Inc; 2012 Mar;Chapter 14:Unit14.11.
64. González JC, Peariso K, Penner-Hahn JE, Matthews RG. Cobalamin-Independent Methionine Synthase from Escherichia coli: A Zinc Metalloenzyme †. Biochem. 1996 Jan;35(38):12228–34.
65. Katzen HM, Buchanan JM. Enzymatic Synthesis of the Methyl Group of Methionine. VIII. Repression-depression, purification, and properties of 5,10-methylene-tetrahydrofolate reductase from *Escherichia coli*. J Biol Chem. 1965 Feb;240:825–35.
66. Chiang PK, Gordon RK, Tal J, Zeng GC, Doctor BP, Pardhasaradhi K, et al. S-Adenosylmethionine and methylation. FASEB J. 1996 Mar;10(4):471–80.
67. Struck A-W, Thompson ML, Wong LS, Micklefield J. ChemInform Abstract: S-Adenosyl-Methionine-Dependent Methyltransferases: Highly Versatile Enzymes in Biocatalysis, Biosynthesis and Other Biotechnological Applications. ChemInform. 2013;44(12):no–no.
68. Turner SJ, Carbone FR, Strugnell RA. Salmonella typhimurium delta aroA delta aroD mutants expressing a foreign recombinant protein induce specific major histocompatibility complex class I-restricted cytotoxic T lymphocytes in mice. Infect Immun. 1993 Dec;61(12):5374–80.
69. Grant SG, Jessee J, Bloom FR, Hanahan D. Differential plasmid rescue from transgenic mouse DNAs into Escherichia coli methylation-restriction mutants. Proc Natl Acad Sci USA. National Academy of Sciences; 1990 Jun;87(12):4645–9.
70. Chang AC, Cohen SN. Construction and characterization of amplifiable multicopy DNA cloning vehicles derived from the P15A cryptic miniplasmid. J Bacteriol. 1978 Jun;134(3):1141–56.
71. Cherepanov PP, Wackernagel W. Gene disruption in Escherichia coli: TcR and KmR cassettes with the option of Flp-catalyzed excision of the antibiotic-resistance determinant. Gene. 1995 May 26;158(1):9–14.
72. Datsenko KA, Wanner BL. One-step inactivation of chromosomal genes in Escherichia coli K-12 using PCR products. Proc Natl Acad Sci USA. 2000 Jun 6;97(12):6640–5.
73. Löber S, Jäckel D, Kaiser N, Hensel M. Regulation of Salmonella pathogenicity island 2 genes by independent environmental signals. Int J Med Microbiol. 2006 Nov;296(7):435–47.

Table 1. Strains and plasmids used for this study.

Strain or plasmid	Relevant phenotypes and genotypes	Source
Strains		
Salmonella enterica Typhimurium SL1344	Wild-type strain *rpsL hisG46*; Str^R	(36)
Salmonella enterica Typhimurium BRD666	Restriction negative modification positive (r^-m^+) SL1344; Str^R	(68)
Escherichia coli DH5α	Cloning strain	(69)
Plasmids		
pGEM-T Easy	High-copy-no. cloning vector for PCR products; Ap^R	Promega
pACBSR	Medium-copy number, mutagenesis plasmid; p15A ori; Ara-inducible I-*Sce*I and λ Red recombinase; Chl^R	(55)
pACYC184	Medium-copy number cloning vector, p15A ori; Tet^R, Chl^R	(70)
pACYC184*metB*	*S.* Typhimurium SL1344 *metB* cloned into pACYC184; Chl^R	This study
pCP20	FLP recombinase, temperature-sensitive replicon; Ap^R, Chl^R	(71)
pKD4	FRT-flanked Km^R cassette; Ap^R, Km^R	(72)

Str, streptomycin; Ap, ampicillin; Chl, chloramphenicol; Km. kanamycin; Ara, arabinose; Flp, flippase; FRT, fippase recombinase target.

Table 2. Oligonucleotide primers used in this study for construction of mutants and complementation.

Mutants	Sequence (5'-3')
Δ*metA*-ISceI-F	TAGGGATAACAGGGTAATCGCCAGTGTTAACGCATGTTC
Δ*metA*-ISceI-R	TAGGGATAACAGGGTAATCGGAATACCACGAATCTGCC
Δ*metA*-Kan-F	**CTAAGGAGGATATTCATATG**CGCAGCCACGGTAATTTACTG
Δ*metA*-Kan-R	**GAAGCAGCTCCAGCCTACACA**ACCTGATAACCTCACGACATACG
Δ*metB*-ISceI-F	TAGGGATAACAGGGTAATCGCAGATCGGCATCATCC
Δ*metB*-ISceI-R	TAGGGATAACAGGGTAATCTTCATCAACCTGCGGCTG
Δ*metB*-Kan-F	**CTAAGGAGGATATTCATATG**CGGTATTGAAGATGGCGAAG
Δ*metB*-Kan-R	**GAAGCAGCTCCAGCCTACACA**CAGCCGTATTGTTCGTCATCG
Δ*metC*-ISceI-F	TAGGGATAACAGGGTAATCCTTCGTTATCTTCGCTGCC
Δ*metC*-ISceI-R	TAGGGATAACAGGGTAATCAGCAGAGTGCGGACAAACG
Δ*metC*-Kan-F	**CTAAGGAGGATATTCATATG**GCTGGTTCGGGTGCATATTG
Δ*metC*-Kan-R	**GAAGCAGCTCCAGCCTACACA**CACTATTCACTGAGCCAAGCG
Δ*metE*-ISceI-F	TAGGGATAACAGGGTAATCTACCTGCGGCCAGCTTG
Δ*metE*-ISceI-R	TAGGGATAACAGGGTAATCAATGCGGTCGCCACTCTG
Δ*metE*-Kan-F	**CTAAGGAGGATATTCATATG**GGCGTTAGCGAACATGGTC
Δ*metE*-Kan-R	**GAAGCAGCTCCAGCCTACACA**TCAACTCGCGACGCAGG
Δ*metF*-ISceI-F	TAGGGATAACAGGGTAATGCAGCCTGATGGAGCATGG
Δ*metF*-SceI-R	TAGGGATAACAGGGTAATGCCACGACCATCAATAGAACG
Δ*metF*-Kan-F	**CTAAGGAGGATATTCATATG**GCCGTGAAGGAGTGAAGGA
Δ*metF*-Kan-R	**GAAGCAGCTCCAGCCTACACA**CTTCCGCCAGGCTCTGATTC
Δ*metH*-ISceI-F	TAGGGATAACAGGGTAATCGGTGAGTCGTGGAATTAGGC
Δ*metH*-ISceI-R	TAGGGATAACAGGGTAATCGTCAGGGCGACAAGATCC
Δ*metH*-Kan-F	**CTAAGGAGGATATTCATATG**GAGGATGTTGAGCGGTGGC
Δ*metH*-Kan-R	**GAAGCAGCTCCAGCCTACACA**GCCGTCCAGCACCAGAATAC
Δ*metNIQ*-ISceI-F	TAGGGATAACAGGGTAATCACAGCTGTGCAGCAGG
Δ*metNIQ*-ISce-R	TAGGGATAACAGGGTAATACTGCCCTGCGGATGG
Δ*metNIQ*-Kan-F	**CTAAGGAGGATATTCATATG**TCCCCTGCTGGAACACTT
Δ*metNIQ*-Kan-R	**GAAGCAGCTCCAGCCTACACA**GTCTGATGAAGTGTACGAAGCC
metB-BamHI-F	TGGATCCGTCGCAGATGTGCGCTAATG
metB-SalI-R	TGTCGACCATAATGCCTGCGACACGC

Endonuclease restriction sites are underlined; kanamycin resistance cassette-specific sequences are in bold; F, forward (5') primer; R, reverse (3') primer.

Table 3. List of metabolites with significantly changes in Δ*metB* mutant compared to wild-type.

XCMS ID	Metabolite name	m/z	Fold change (Δ*metB* to WT)	*p*-value	FDR
M900T1200	4-Hydroxyphenylacetyl-CoA	900.15	3247.21	4.17E-07	4.01E-05
M878T1201	UDP-N-acetylmuramoyl-L-alanyl-D-glutamate	878.17	1646.67	7.63E-08	1.45E-05
M880T1200	3-Hydroxyhexanoyl CoA	880.18	220.30	6.08E-07	5.15E-05
M749T1087	UDP-N-acetylmuramoyl-L-alanine	749.13	12.24	7.22E-06	2.49E-04
M163T480	Rhamnose	163.06	10.30	3.99E-08	1.33E-05
M275T1210	6-Phosphogluconate	275.02	8.93	1.01E-04	1.74E-03
M105T825	D-Glycerate	105.02	8.15	8.18E-06	2.67E-04
M259T1165	Hexose-Phosphate	259.02	7.36	7.32E-04	8.43E-03
M266T579	Adenosine	266.09	6.13	1.44E-04	2.33E-03
M195T999	Gluconate	195.05	6.13	7.04E-07	5.68E-05
M1050T1225	UDP-N-acetylmuramoyl-L-alanyl-D-γ-glutamyl-meso-2,6- diaminopimelate	1050.26	5.63	1.75E-06	9.97E-05
M189T1246	Diaminoheptandioate	189.09	4.73	6.05E-07	5.15E-05
M620T1224	UDP-N-acetyl-2-amino-2-deoxy-D-glucuronate	620.05	4.67	9.09E-09	7.57E-06
M134T607	Adenine	134.05	4.44	6.48E-06	2.31E-04
M686T707	Dephospho-CoA	686.14	4.22	1.36E-05	3.75E-04
M218T1006	O-Succinyl-L-homoserine	218.07	3.75	5.85E-05	1.14E-03
M145T567	2-Dehydropantoate	145.05	3.72	2.60E-05	6.15E-04
M130T567	hydoxy-proline	130.05	3.19	2.46E-04	3.57E-03
M273T1080	Succinyl-Arginine	273.12	2.55	1.28E-04	2.11E-03
M678T1139	UDP-N-acetylmuraminate	678.09	2.45	1.41E-07	2.10E-05
M227T987	4-Phosphopantoate	227.03	2.11	3.55E-04	4.74E-03
M116T860	Valine	116.07	2.03	1.21E-04	2.02E-03

This table presents results from a one-way ANOVA performed with Tukey's honest significant difference (HSD) tests ($p<0.01$). FDR, false discovery rate.

Figure legends

Figure 1. Schematic diagram of the biosynthetic pathway of Met in *S.* Typhimurium. The first committed step of the pathway is catalysed by homoserine transsuccinylase (MetA), which succinylates homoserine to form O-succinyl L-homoserine, which then undergoes a condensation reaction with cysteine to form L-cystathionine, catalysed by cystathionine γ-synthase (MetB). Cystathionine β-lyase (MetC) catalyses the conversion of L-cystathionine to L-homocysteine, pyruvate and ammonia. The final biosynthetic step is catalysed by distinct Met synthases, MetH and MetE, which are vitamin B12-dependent and -independent synthases, respectively (31,32,64). In this final step, L-homocysteine is condensed with 5,10-methyltetrahydrofolate (CH_3H_4Folate), which donates the methyl group. CH_3H_4Folate is provided from the one-carbon cycle through a methylenetetrahydrofolate reductase (MetF)-mediated reaction, producing tetrahydrofolate (H_4Folate) and Met (65). In *S. enterica*, Met is recycled through an activated methyl cycle. The primary methyl donor S-adenosyl methionine (SAM) is formed by the activation of Met through an ATP-dependent condensation reaction catalyzed by the S-adenosyl methionine synthase (MetK)(2,66,67). Catalytic enzymes are in red; arrows indicate the direction of catalytic reactions.

Figure 2. The *de novo* biosynthetic mutants demonstrate Met-dependent growth in M9 minimal media and in HeLa cells, but remain fully virulent in mice. *S.* Typhimurium wild-type (WT) SL1344 and mutant strains were grown shaking at 37°C in M9 minimal media with or without A) Met, B) vitamin B12, or C) oxygen, and the number of viable bacteria (cfu) was determined after 24 hours. Bars represent the mean cfu and error bars show the data range. Dotted lines represent the bacterial concentration at the time of inoculation. Data are pooled from two independent experiments. D) The *de novo* Met biosynthetic mutants become defective for intracellular replication in HeLa cells when Met is absent in the DMEM media. HeLa cells were grown to a monolayer and infected with *S.* Typhimurium WT or mutant strains at a multiplicity of infection (MOI) of 5-10, in Met-free DMEM. The intracellular bacterial load at 2 hours post-infection is expressed as "1" and used as the reference point to calculate fold-change of intracellular bacterial number at subsequent time points. Data are pooled from three independent experiments. Bars represent the mean cfu and error bars show the data range. Unpaired *t*-tests were used to compare the intracellular load of WT and mutant strains at 10 hours post-infection, and *p*-values shown were corrected for multiple comparisons using the Bonferroni-Dunn method; *p*-values greater than 0.05 were deemed as not significant (ns). For assessing virulence *in vivo*, age- and sex-matched C57BL/6 mice were intravenously infected with 200 cfu of indicated strains of *S.* Typhimurium, and the bacterial load in the E) liver and F) spleen was determined at day 5 post-infection. Symbols represent data from individual animals, and horizontal lines represent the geometric mean of each group. Data are pooled from two independent experiments. One-way ANOVA with Bonferroni post-tests was used for statistical analyses comparing each pair of data groups, and none of the comparisons yielded a *p*-value below 0.05.

Figure 3. *S.* Typhimurium mutants deficient in the *de novo* biosynthesis and high-affinity transport of Met are highly attenuated in mice. A) *S.* Typhimurium strains were grown shaking at 37°C in M9 minimal media with or without Met, and the number of viable bacteria (cfu) was determined after 24 hours. Bars represent the mean cfu and error bars show the data range. Dotted lines represent the bacterial concentration at the time of inoculation. Data are pooled from two independent experiments. B) HeLa cells were grown to a monolayer and infected with *S.* Typhimurium WT or mutant strains at a multiplicity of infection (MOI) of 5-10, in DMEM media with or without Met. The intracellular bacterial load at 2 hours post-infection is expressed as "1" and used as the reference point to calculate fold-change of intracellular bacterial number at subsequent time points. Bars represent the mean cfu and error bars show the data range. Data are pooled from three independent experiments. Unpaired *t*-tests were used to compare the intracellular load of WT and mutant strains at 10 hours post-infection, and *p*-values shown were corrected for multiple comparisons using the Bonferroni-Dunn method; *p*-values greater than 0.05 were deemed as not significant (ns). For assessing virulence *in vivo*, age- and sex-matched C57BL/6 mice were intravenously infected with 200cfu of indicated strains of *S.* Typhimurium, and the bacterial load in the D) liver and E) spleen was determined at day 5 post-infection. Δ*metNIQ*Δ*metB*/p*metB*-c' denotes the complemented strain Δ*metNIQ*Δ*metB* pACYC184*metB*. Symbols represent data from individual animals,

and horizontal lines represent the geometric mean of each group. Data are pooled from three independent experiments. One-way ANOVA with Bonferroni post-tests was used for statistical analyses, ****, $p<0.0001$; ns, $p>0.05$.

Figure 4. Metabolite perturbations following genetic disruption to Met biosynthesis, one-carbon cycle and activated methyl cycle. Total metabolite pools in each strain were detected and quantitated using LC-QTOF (Liquid Chromatography-Quadrupole Time-of-flight). Key intermediates of the Met biosynthetic pathway, activated methyl cycle and one-carbon cycle were identified and quantified for the indicated *S.* Typhimurium strains, and compared to the wild-type level; fold-changes are shown for A) 5-methyltetrahydropteroyltri-L-glutamate, a member of the polyglutamate forms of 5-methyltetrahydrofolate, B) O-succinyl homoserine, C) Met and D) SAM. Δ*metNIQ*Δ*metB*/p*metB*-c' denotes the complemented strain Δ*metNIQ*Δ*metB* pACYC184*metB*. Individual data points represent biological replicates, and the mean for each group is shown. One-way ANOVA with Bonferroni post-tests were used to compare the metabolite level in each mutant to wild-type, *p*-values <0.05 are shown: *, $p<0.05$; **, $p<0.01$; ***, $p<0.001$; and ****, $p<0.0001$.

Figure 5. Metabolite perturbations following genetic disruption to *metB*, *metE* and *metH*. Scatter plots depict wild-type compared to A) Δ*metB*, B) Δ*metE* and C) Δ*metH*. Each dot represents a single extracted m/z feature with each axis depicting the arbitrary ion count. m/z features which are no different between conditions plot along the diagonal. The colour intensity indicates the confidence of the difference (greater intensity equates to lower variance across biological replicates). Yellow highlight indicates a subset of confirmed metabolites with a statistically significant difference in a pair-wise comparison ($p<0.05$ with Benjamini correction). D) The levels of four metabolites associated with peptidoglycan synthesis were significantly altered in Δ*metB* and Δ*metNIQ*Δ*metB* mutants. UDP-MurNAc, UDP-N-acetyl-muraminate; UDP-MurNAc-L-Ala, UDP-N-acetyl-muramoyl-L-alanine; UDP-MurNAc-L-Ala-D-Glu, UDP-N-acetyl-muramoyl-L-alanyl-D-glutamate; and UDP-MurNAc-L-Ala-γ-D-Glu-*m*-DAP, UDP-N-acetyl-muramoyl-L-alanyl-D-glutamyl-*meso*-diaminopimelate. Δ*metNIQ*Δ*metB*/p*metB*-c' denotes the complemented strain Δ*metNIQ*Δ*metB* pACYC184*metB*. Individual data points represent biological replicates, and the mean for each group is shown. One-way ANOVA with Bonferroni post-tests were used to compare the metabolite level in each mutant to wild-type, *p*-values <0.05 are shown: *, $p<0.05$; **, $p<0.01$; ***, $p<0.001$; and ****, $p<0.0001$.

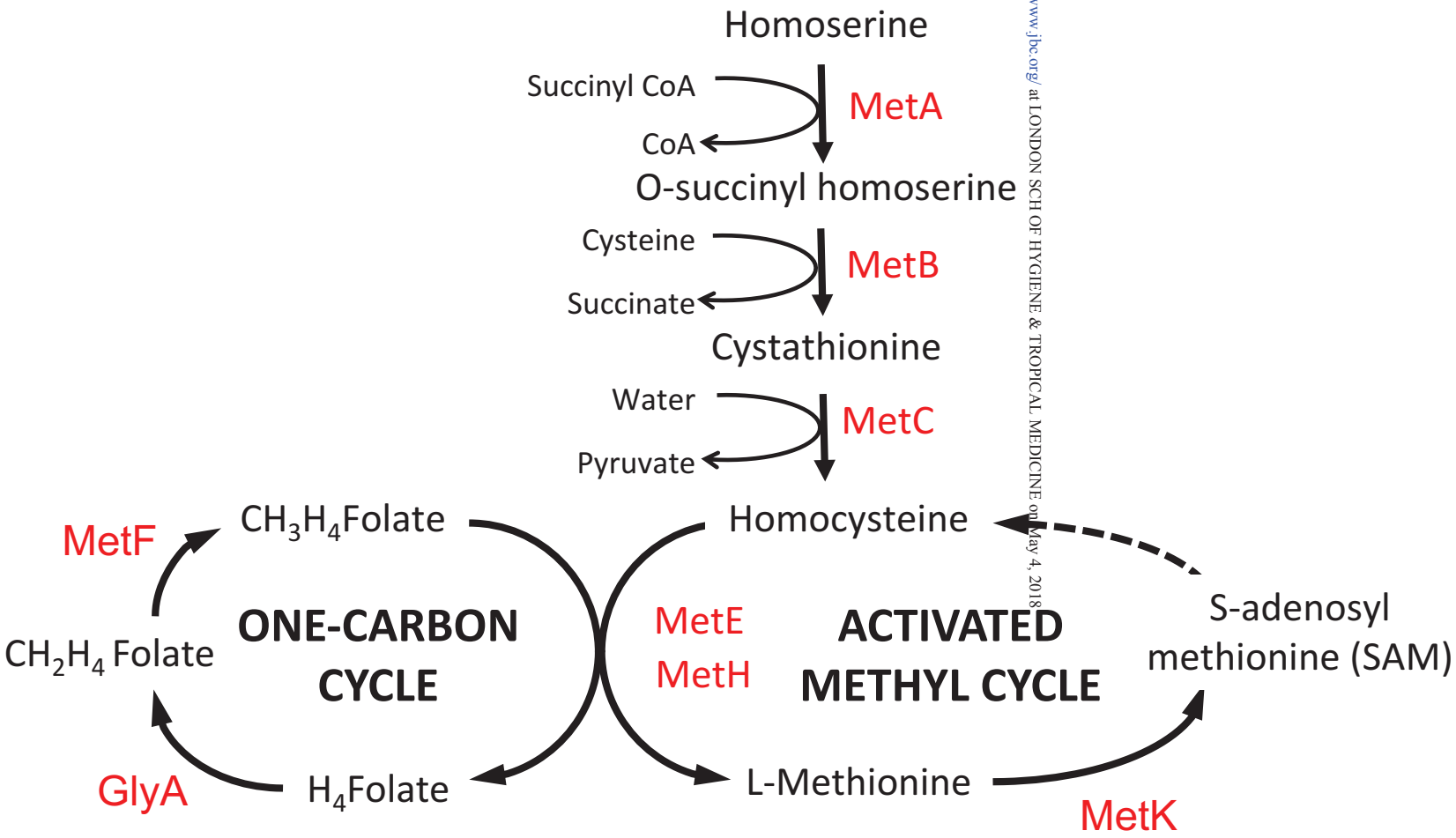

Figure 1

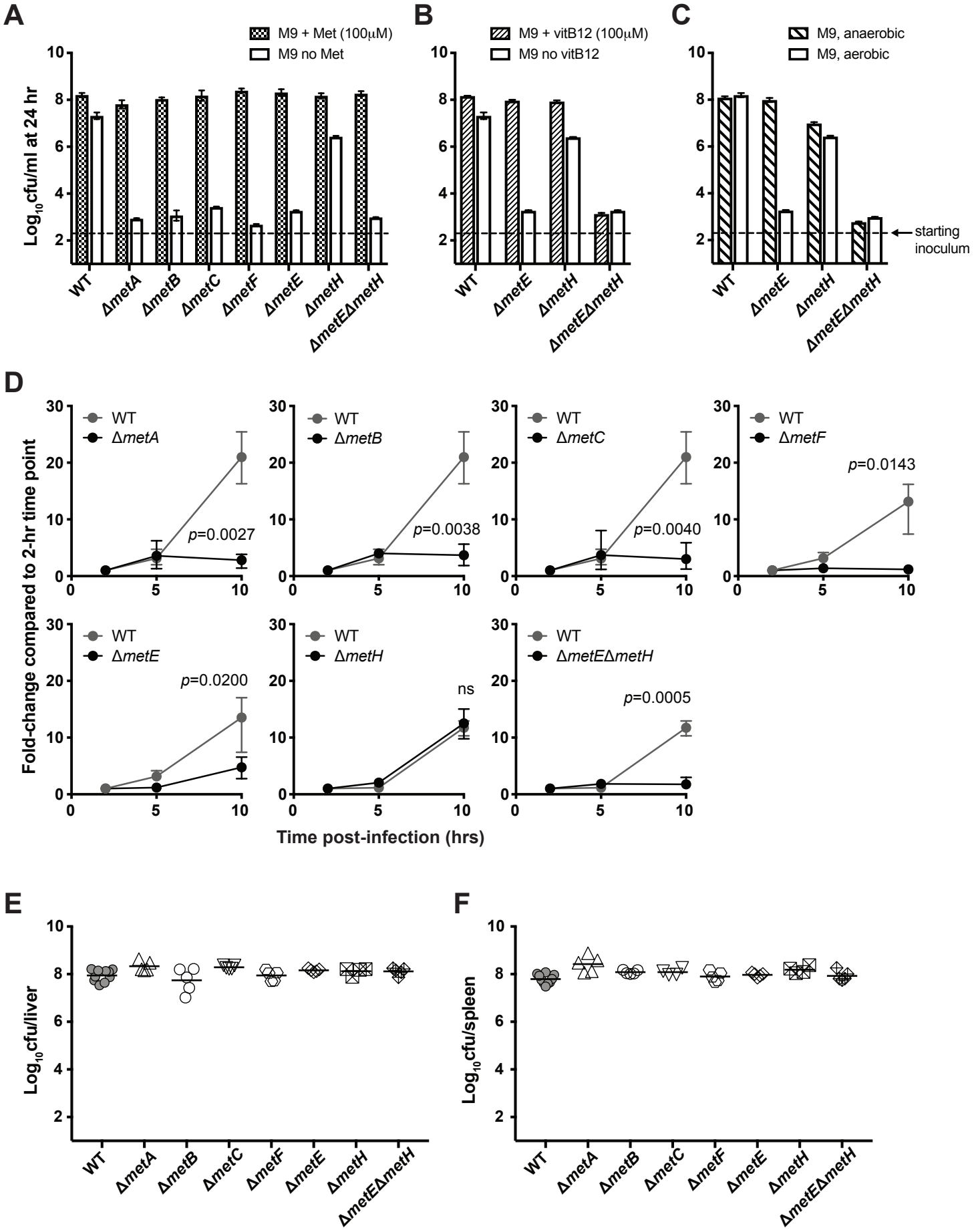
A
M9 + Met (100μM)
M9 no Met
Log10 cfu/ml at 24 hr
WT
ΔmetA
ΔmetB
ΔmetC
ΔmetF
ΔmetE
ΔmetH
ΔmetEΔmetH
B
M9 + vitB12 (100μM)
M9 no vitB12
C
M9, anaerobic
M9, aerobic
starting inoculum
D
Fold-change compared to 2-hr time point
p=0.0027
p=0.0038
p=0.0040
p=0.0143
p=0.0200
ns
p=0.0005
Time post-infection (hrs)
E
Log10 cfu/liver
F
Log10 cfu/spleen

Figure 2

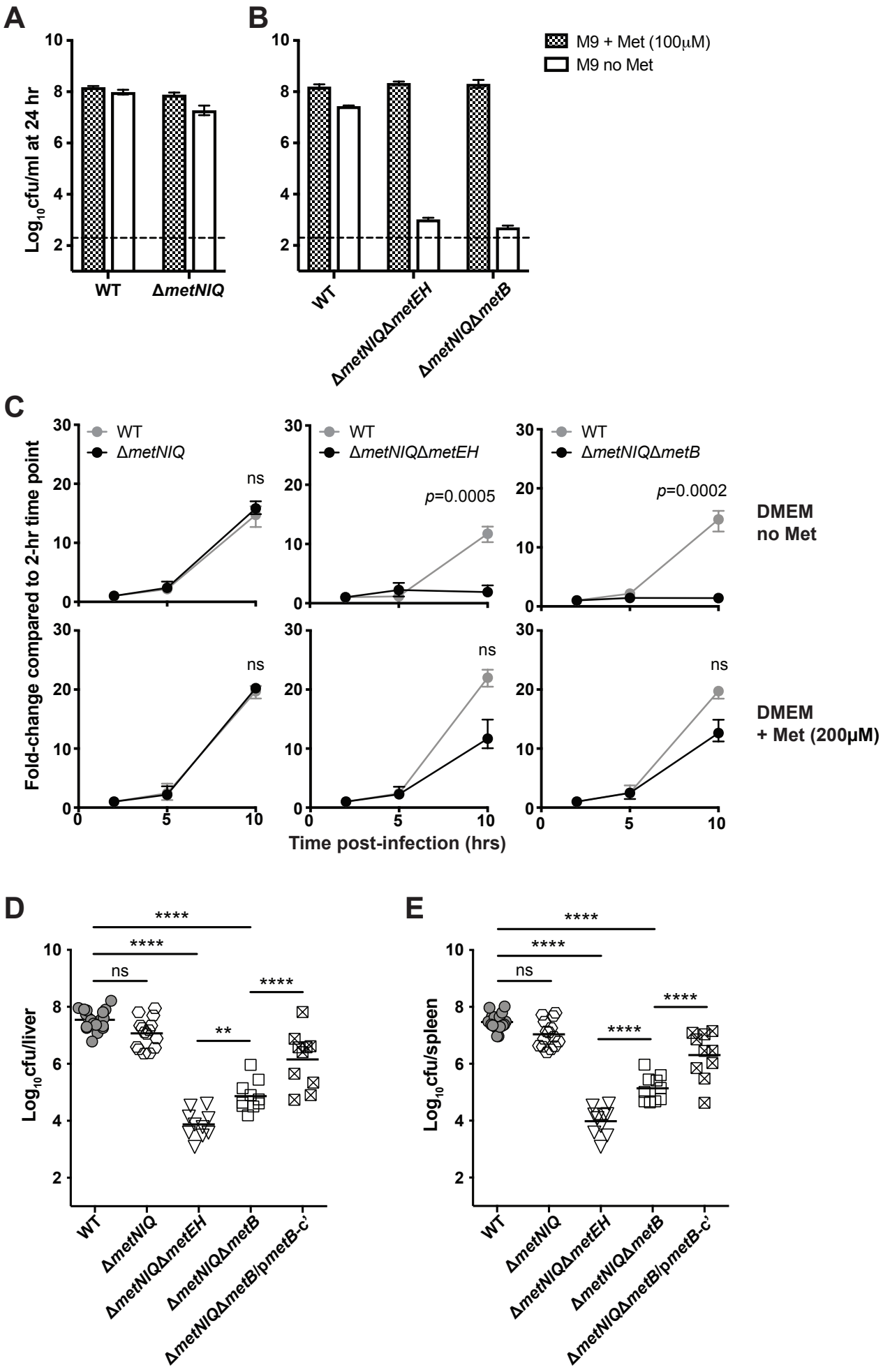
A
B
M9 + Met (100μM)
M9 no Met
Log10cfu/ml at 24 hr
WT
ΔmetNIQ
ΔmetNIQΔmetEH
ΔmetNIQΔmetB
C
WT
ΔmetNIQ
ΔmetNIQΔmetEH
ΔmetNIQΔmetB
ns
p=0.0005
p=0.0002
DMEM
no Met
DMEM
+ Met (200μM)
Fold-change compared to 2-hr time point
Time post-infection (hrs)
D
E
****
ns
**
Log10cfu/liver
Log10cfu/spleen
ΔmetNIQ/pmetB-c'

Figure 3

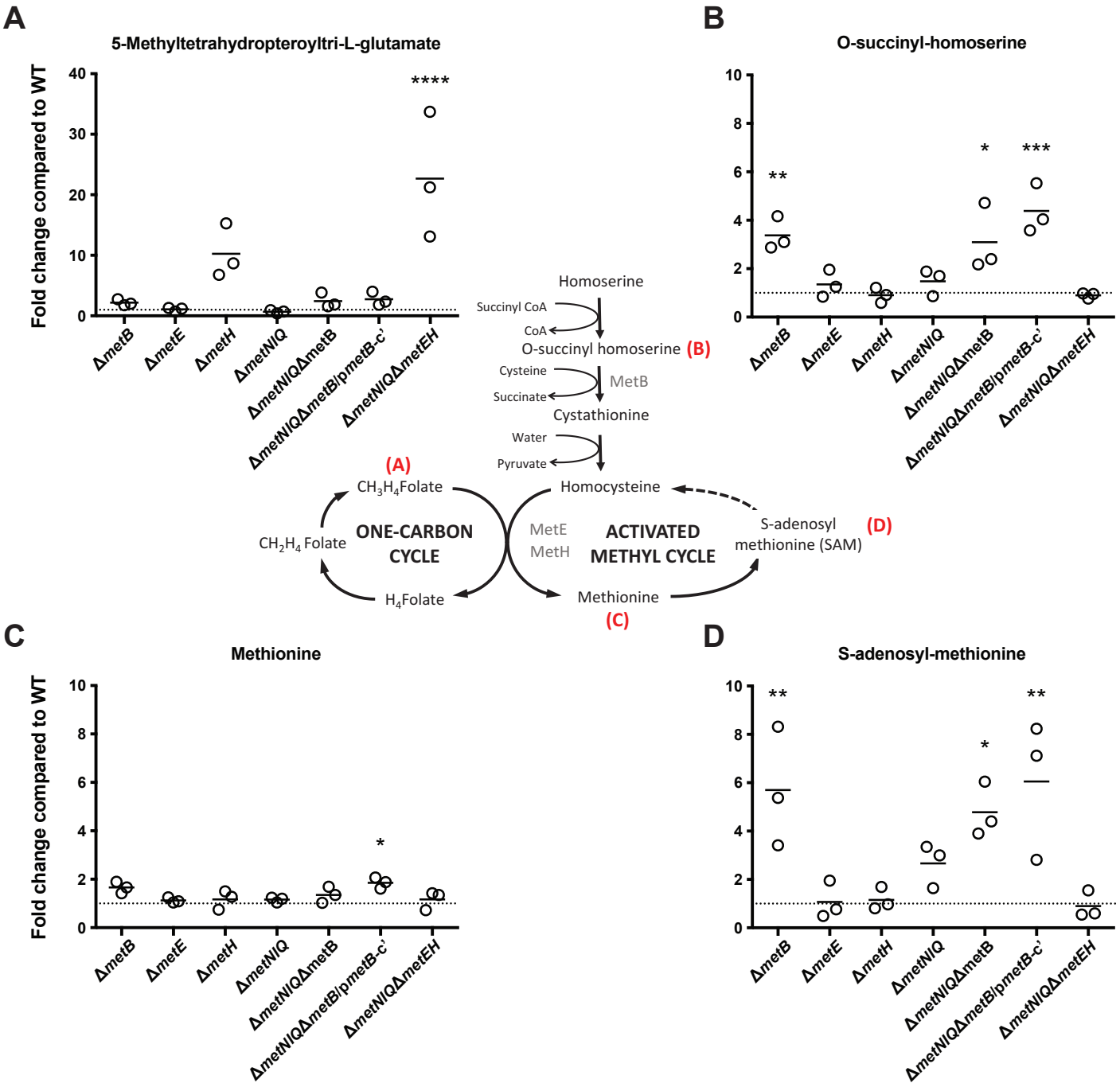
A
5-Methyltetrahydropteroyltri-L-glutamate
Fold change compared to WT
40
30
20
10
0
****
ΔmetB
ΔmetE
ΔmetH
ΔmetNIQ
ΔmetNIQΔmetB
ΔmetNIQΔmetB/pmetB-c'
ΔmetNIQΔmetEH
B
O-succinyl-homoserine
10
8
6
4
2
0
**
*
***
ΔmetB
ΔmetE
ΔmetH
ΔmetNIQ
ΔmetNIQΔmetB
ΔmetNIQΔmetB/pmetB-c'
ΔmetNIQΔmetEH
Homoserine
Succinyl CoA
CoA
O-succinyl homoserine (B)
Cysteine
Succinate
MetB
Cystathionine
Water
Pyruvate
(A)
CH3H4Folate
Homocysteine
CH2H4 Folate
ONE-CARBON CYCLE
MetE
MetH
ACTIVATED METHYL CYCLE
S-adenosyl methionine (SAM)
(D)
H4Folate
Methionine
(C)
C
Methionine
Fold change compared to WT
10
8
6
4
2
0
*
ΔmetB
ΔmetE
ΔmetH
ΔmetNIQ
ΔmetNIQΔmetB
ΔmetNIQΔmetB/pmetB-c'
ΔmetNIQΔmetEH
D
S-adenosyl-methionine
10
8
6
4
2
0
**
*
**
ΔmetB
ΔmetE
ΔmetH
ΔmetNIQ
ΔmetNIQΔmetB
ΔmetNIQΔmetB/pmetB-c'
ΔmetNIQΔmetEH

Figure 4

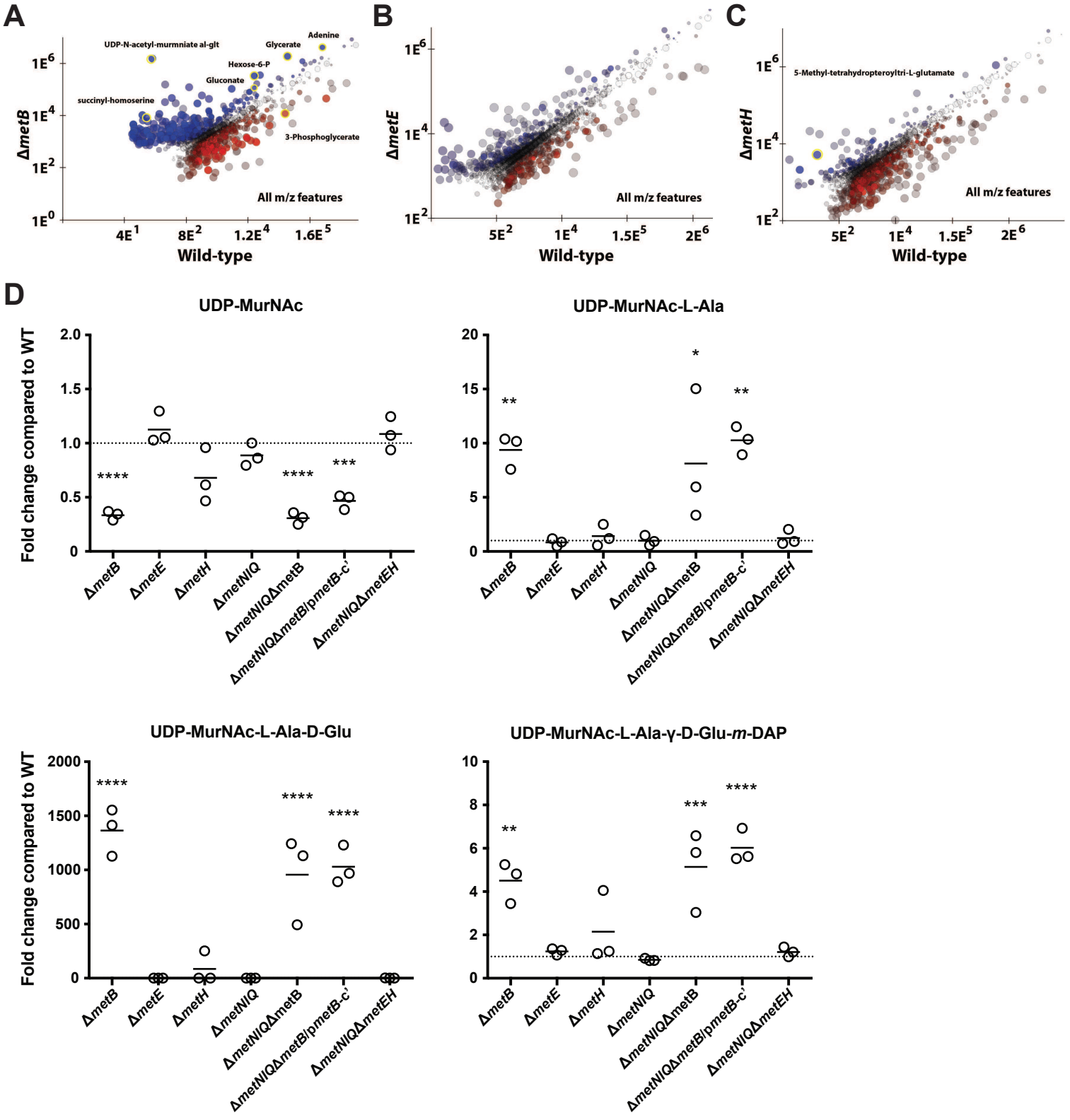
A
B
C
D
ΔmetB
ΔmetE
ΔmetH
Wild-type
All m/z features
UDP-N-acetyl-murmniate al-glt
Glycerate
Adenine
Hexose-6-P
Gluconate
succinyl-homoserine
3-Phosphoglycerate
5-Methyl-tetrahydropteroyltri-L-glutamate
UDP-MurNAc
UDP-MurNAc-L-Ala
UDP-MurNAc-L-Ala-D-Glu
UDP-MurNAc-L-Ala-γ-D-Glu-m-DAP
Fold change compared to WT
ΔmetB
ΔmetE
ΔmetH
ΔmetNIQ
ΔmetNIQΔmetB
ΔmetNIQΔmetB/pmetB-c'
ΔmetNIQΔmetEH

Figure 5

Methionine biosynthesis and transport are functionally redundant for the growth and virulence of *Salmonella* Typhimurium

Asma Ul Husna, Nancy Wang, Simon A. Cobbold, Hayley J. Newton, Dianna M. Hocking, Jonathan J. Wilksch, Timothy A. Scott, Mark R. Davies, Jay C. Hinton, Jai J. Tree, Trevor Lithgow, Malcolm J. McConville and Richard Strugnell

J. Biol. Chem. published online May 2, 2018
